07

Asymptotic solutions of equations for P- and Q-distributions in the model of a single-atom laser with incoherent pumping

© N.V. Larionov[1,2]

[1] State Marine Technical University, St. Petersburg, Russia
[2] Peter the Great Saint-Petersburg Polytechnic University, St. Petersburg, Russia

e-mail: larionov.nickolay@gmail.com

Received May 31, 2025
Revised November 07, 2025
Accepted November 11, 2025

The steady-state operation of a single-atom laser with incoherent pumping is investigated based on equations for phase-averaged P and Q distributions. It is shown that under the conditions of the existence of a semiclassical solution, a large parameter appears in these equations, which makes it possible to obtain their approximate solutions. The latter contain the main asymptotic solutions obtained earlier and describe the operation of a single-atom laser on two characteristic scales of the problem: „linear", when a single-atom laser can generate like a conventional laser, and „square-law", when the Fermi statistics of a single-atom are significant. It is shown that for the introduced „linear"scale of the problem, the P distribution of a single-atom laser coincides with the corresponding distribution for a laser with a macroscopic number of emitters. The conditions for the thresholdless operation of a single-atom laser have been clarified.

Keywords: single-atom laser, quasi-probability distribution, strong coupling regime, sub-Poisson statistics, two-level atom, thresholdless regime.

DOI: 10.61011/EOS.2026.01.63222.8230-25

1. Introduction

The single-atom laser is one of the fundamental models in quantum optics [1–24]. The simplest variation of this model is represented by a two-level atom with incoherent pumping which interacts with a damped single-mode cavity field.

For this model, a stationary solution for the intra-cavity intensity [1] is known (we'll call this solution „semiclassical"), which demonstrates a distinctive feature of a single-atom laser: the square-law dependence of the intracavity intensity on the pump parameter, describing the transition to self-quenching after saturation.

Some works devoted to the study of this single-atom laser problem are based on the analysis of the density operator equation written in the coherent state representation. Thus, the authors in [9,10,14,15,19,23], considering various limiting cases in the steady-state laser operation and find approximate expressions for the phase-averaged Glauber–Sudarshan P-distributions and Q-Husimi distributions (hereinafter P- and Q-distributions). The obtained expressions complement the semiclassical solution and, in particular, describe the transition to thresholdless laser operation and sub-Poisson photon statistics in the case of atom-field strong coupling. In this case, the P-distribution is mainly represented by non-analytical functions with a limited domain of definition.

The differences in approaches from different authors are insignificant and consist in the fact that in one case [9,10], a system of first-order differential equations is analyzed for various auxiliary distributions (conditional probabilities), and in the other [14,23] — a single differential equation is analyzed either for P-distribution, or for Q-distribution.

Under the conditions of existence of semiclassical solution the differential equation for P-distribution [14] it is an equation with a small parameter at the highest derivative. The solution that was found in [14] can be interpreted from the point of view of perturbation theory as a solution to the „unperturbed" equation, which is also called the WKB approximation [25]. With its help, the behavior of a single-atom laser in a wide range of pump parameter values was investigated, and the case of a high-Q cavity, previously considered in [9], was described more precisely.

In this paper, it will be shown that the case of the extremely strong atom-field coupling outlined from [10], is also described by a solution in [14]. In this case, an additional condition will be found, under which this solution will coincide with the solution for a conventional laser with a macroscopic number of emitters [26].

The behavior of a single-atom laser near a semi-classical threshold will be analyzed separately. The transition to the thresholdless regime during the transition from the case of weak atom-field coupling to the case of extremely strong atom-field coupling will be consistently considered.

In papers [19,23], similar to [14], differential equation for Q-distribution is obtained. Under the conditions of existence of semiclassical solution this equation will have its approximated solution [23], allowing to reproduce the results from [14]. And for the case of atom-field strong coupling regime it is possible to delineate a weak sub-Poissonian photon statistics earlier mentioned in [12]. At

that, P-distribution from [14] due to its quasi-probabilistic properties, did not allow to describe this feature.

Yet, the expression obtained for Q-distribution [23] doesn't cover the case of extremely strong atom-field coupling [10]. Therefore, this study will be focused on finding the connection between the solutions from [10] and [23].

The study is structured as follows. The second section presents a theoretical model of a single-atom laser. The initial equations for the phase-averaged P- and Q-distributions are given and the conditions under which they are analyzed are specified. The following sections are focused on finding a small parameter in these equations, the search and analysis of the corresponding asymptotic solutions. The findings are summarized in the last section. The appendix contains some bulky formulas and coefficients from equations.

2. Theoretical model

The equation for the density operator $\hat{\rho}$ of a single-atom laser has the following form [27]:

$$\frac{\partial\hat{\rho}}{\partial t} = -\frac{i}{\hbar}[\hat{V},\hat{\rho}] + \frac{\kappa}{2}\left(2\,\hat{a}\hat{\rho}\hat{a}^{\dagger} - \hat{a}^{\dagger}\hat{a}\hat{\rho} - \hat{\rho}\hat{a}^{\dagger}\hat{a}\right) + \frac{\gamma}{2}\left(2\hat{\sigma}\hat{\rho}\hat{\sigma}^{\dagger} - \hat{\sigma}^{\dagger}\hat{\sigma}\hat{\rho} - \hat{\rho}\hat{\sigma}^{\dagger}\hat{\sigma}\right) + \frac{\Gamma}{2}\left(2\hat{\sigma}^{\dagger}\hat{\rho}\hat{\sigma} - \hat{\sigma}\hat{\sigma}^{\dagger}\hat{\rho} - \hat{\rho}\hat{\sigma}\hat{\sigma}^{\dagger}\right). \quad (1)$$

Here, $\hat{a}$ and $\hat{a}^{\dagger}$ — photon annihilation and creation operators in the cavity mode, $\hat{\sigma} = |1\rangle\langle 2|$ and $\hat{\sigma}^{\dagger} = |2\rangle\langle 1|$ — atom transitions operators where $|1\rangle$, $|2\rangle$ — the vectors of the ground and excited states of the atom, respectively.

The first term in (1) describes the interaction of the single cavity mode with a two-level atom according to the Jaynes–Cummings Hamiltonian with the coupling constant g:

$$\hat{V} = i\hbar g\left(\hat{a}^{\dagger}\hat{\sigma} - \hat{\sigma}^{\dagger}\hat{a}\right). \quad (2)$$

The second and third terms take into account the cavity mode decay at a rate of $\kappa/2$ and the spontaneous decay of an atom at a rate of $\gamma/2$, respectively. The last term is related to the incoherent pumping of an atom from the lower level $|1\rangle$ to the upper level $|2\rangle$ at a rate of $\Gamma/2$.

To describe the operation of a single-atom laser, we introduce the following three dimensionless parameters: $r = \Gamma/\gamma$ — pumping rate, $I_s = \gamma/\kappa$ — saturation coefficient and $c = 4g^2/\kappa\gamma$ — coupling constant (cooperative parameter).

2.1. Equations for the phase-averaged P- and Q-distributions

As shown in [14,19,23], from equation (1), in the steady-state, it is possible to obtain linear homogeneous differential equations with polynomial coefficients for phase-averaged P- and Q-distributions.

Thus, for the P-distribution this is a second-order equation

$$\sum_{\nu=0}^{2} p_{2-\nu}(I)P^{(\nu)}(I) = 0, \quad (3)$$

where the designation $P^{(\nu)}(I) \equiv d^{\nu}P(I)/dI^{\nu}$ and the distribution depends only on the intensity variable $I = |z|^2$, which is the square of the modulus of the complex number $z = \sqrt{I}e^{i\varphi}$.

The polynomials in (3) are expressed as

$$\begin{aligned} p_0(I) &= I^2(I - I_0), \\ p_1(I) &= a_{12}(I - I_{-1})(I - I_{+1}), \\ p_2(I) &= a_{22}(I - I_{-2})(I - I_{+2}), \end{aligned} \quad (4)$$

where the roots of polynomials I_0, $I_{\pm1,\pm2}$ and coefficients a_{12}, a_{22} depend on the laser parameters r, I_s, c. The entries of the polynomials in their canonical form $(a_{i0} + a_{i1}I + a_{i2}I^2)$ and the explicit form of the coefficients a_{ik} are given in Appendix 1.

Note that one of the main problems encountered when finding a solution to equation(3) is that the ratio p_1/p_0 for $I = 0$ goes to infinity as I^{-2} [28].

The differential equation for Q-distribution will be of the fifth order:

$$\sum_{\nu=0}^{5} q_{5-\nu}(I)Q^{(\nu)}(I) = 0, \quad (5)$$

where polynomials

$$\begin{aligned} q_0(I) &= I^2(I - I_{00}), \\ q_1(I) &= 3I(I - I_{11})(I - I_{12}), \\ q_2(I) &= 3(I - I_{21})(I - I_{22})(I - I_{23}), \\ q_3(I) &= (I - I_{31})(I - I_{32})(I - I_{33}), \\ q_4(I) &= b_{42}(I - I_{41})(I - I_{42}), \\ q_5(I) &= b_{52}(I - I_{51})(I - I_{52}). \end{aligned} \quad (6)$$

The canonical form of these polynomials is also given in Appendix 1.

2.2. Semiclassical solution. Mandel Q_f parameter

As reference solutions, we will use a semiclassical solution for stationary intracavity intensity [1,12]

$$I_{\text{int}} = \frac{I_s}{2}\left[(r-1) - \frac{(r+1)^2}{c}\right] \quad (7)$$

and the expression for Mandel Q_f parameter obtained after linearization of Heisenberg–Langevin equations [12,14]

near I_{int} (7)

$$Q_f = \frac{\langle \hat{n}^2 \rangle - \langle \hat{n} \rangle^2}{\langle \hat{n} \rangle} = \frac{r}{\left[(r-1) - \frac{(r+1)^2}{c} \right]} - \frac{3(r+1)}{2c} - 1, \tag{8}$$

where $\hat{n} = \hat{a}^\dagger \hat{a}$ — photon number operator.

Expressions (7), (8) are true when $c > 8$ and r lie between the pumping threshold value r_{th} and the value r_q corresponding to the self-quenching effect:

$$\begin{aligned} & r_{\text{th}} < r < r_q, \\ & r_{\text{th}} = r_{\max} - \frac{c}{2}\sqrt{1 - 8/c}, \\ & r_q = r_{\max} + \frac{c}{2}\sqrt{1 - 8/c}, \end{aligned} \tag{9}$$

where $r_{\max} = c/2 - 1$ is the pumping rate at which I_{int} (7) reaches its maximum

$$I_{\max} = \frac{cI_s}{8}\,(1 - 8/c)\,. \tag{10}$$

As mentioned earlier, the best match of analytical solutions (7), (8) with numerical analysis occurs in case of a „good“ cavity $I_s \gg 1$.

2.3. Conditions applied

Now we will determine the characteristic values of the laser parameters, at which we will investigate the equations for P- and Q-distributions.

If it is not specifically specified, then we will assume that the following conditions are met:

$$cI_s \gg 8, \quad c \gg 8. \tag{11}$$

The fulfillment of these conditions, which we will call the conditions for the existence of a semiclassical solution (7), allows us to accumulate a large number of coherent photons in the cavity mode.

Let's consider two possible cases: 1) $c > I_s$ — strong atom-field, coupling when the coupling of the atom to the cavity mode is stronger than the coupling of the atom to the reservoir responsible for its spontaneous decay; 2) $c < I_s$ — reverse case — weak atom-field coupling.

The limiting cases of strong and weak atom-field couplings will have the following limiting transitions: $c \to \infty$ and $I_s \to \infty$.

The solution (8) predicts the weak sub-Poissonian behavior of laser[1], which exists for $c > 200$ near the value $r = c/5$ ($r_{\text{th}} \ll c/5 < r_{\max}$). In the limit $c \to \infty$, $Q_f \approx -0.05$. It is near these parameters that P-distribution strongly exhibits its quasi-probabilistic properties [14,15].

3. P- and Q-distributions under conditions of existence of a semiclassical solution

Let the condition for the existence of a semiclassical solution (11) be fulfilled, then, in equations (3) and (5) there's a large parameter $\lambda = cI_s$ (see coefficients in Appendix 1, a_{22} (A2), b_{52} (A4)).

Let's introduce the characteristic scale of the problem I_{sc} and rewrite the equations (3) and (5) via the new variable $x = I/I_{sc}$. Then the equation for P-distribution will be expressed as:

$$\begin{aligned} & x^2 (x - x_0) P^{(2)}(x) - \lambda\alpha (x - x_{-1})(x - x_{+1}) P^{(1)}(x) \\ & \quad + \lambda I_{sc} (x - x_{-2})(x - x_{+2}) P(x) = 0, \end{aligned} \tag{12}$$

where $x_0 = I_0/I_{sc}$, $x_{\pm 1,2} = I_{\pm 1,2}/I_{sc}$ and it was taken into account that $a_{12} = -\alpha\lambda$, $\alpha = [1 + 3(r+1)/2c]$ and $a_{22} = \lambda$.

Equation for Q-distribution:

$$\begin{aligned} & I_{sc}^{-3} x^2 (x - x_{00}) Q^{(5)}(x) + 3I_{sc}^{-2} x (x - x_{11})(x - x_{12}) \\ & \times Q^{(4)}(x) + 3I_{sc}^{-1} (x - x_{21})(x - x_{22})(x - x_{23}) Q^{(3)}(x) \\ & + (x^3 + I_{sc}^{-3} b_{30}) Q^{(2)}(x) + \lambda I_{sc}^{-1} \left(\tilde{b}_{32} x^2 + I_{sc}^{-1} \tilde{b}_{31} x \right) \\ & \times Q^{(2)}(x) + \lambda\beta (x - x_{41})(x - x_{42}) Q^{(1)}(x) \\ & + \lambda I_{sc} (x - x_{51})(x - x_{52}) Q(x) = 0, \end{aligned} \tag{13}$$

where it was taken into account that $b_{42} = \lambda\beta$, $b_{52} = \lambda$ and $\beta = [2 - 3(r+1)/2c]$ and designations $\tilde{b}_{31} = b_{31}/\lambda$, $\tilde{b}_{32} = b_{32}/\lambda$ were introduced.

3.1. „Square-law“ characteristic scale

3.1.1. „Unperturbed“ solution for P-distribution

Let's set the following characteristic scale $I_{sc} = cI_s/8 \approx I_{\max}$ (10), which we will call a „square-law“, assuming a square-law dependence of I_{int} (7) on the pumping parameter.

Analyzing the polynomials in (12), we can show that under the conditions of (11), in particular, when the pumping parameter is comparable to the cooperative parameter $r \sim c$, the roots of the polynomials are $x_0, x_{\pm 1,2} \sim 1$.

As can be seen from (12), the highlighted large parameter λ allows us to consider the equation for the P-distribution as an equation with a small parameter at the highest derivative [25,29]. Removing the term with $1/\lambda$ in (12),

[1] In [12] all numerical calculations confirming the expressions (7), (8), were carried out using equation (3), which was later published in [14]. At the same time, due to the quasi-probabilistic properties of P-distribution, the calculation area was limited to the root I_{-1}. That is why the sub-Poissonian property, which is predicted by the expression (8), is discussed later in [14,23].

we obtain a „unperturbed“ equation, the solution of which has the form

$$P_0(I) = \begin{cases} N_0(I_{-1}-I)^{f_1}(I_{+1}-I)^{f_2}e^{I/\alpha}, & I \leqslant I_{-1}, \\ 0, & I > I_{-1}, \end{cases} \quad (14)$$

where N_0 is a normalization constant and a transition was made back to variable intensity I and the roots $I_{\pm1}$, $I_{\pm2}$. Powers in (14):

$$f_1 = \frac{(I_{-1}-I_{-2})(I_{-1}-I_{+2})}{\alpha(I_{-1}-I_{+1})},$$

$$f_2 = -\frac{(I_{+1}-I_{-2})(I_{+1}-I_{+2})}{\alpha(I_{-1}-I_{+1})}. \quad (15)$$

The solution (14) was obtained earlier in [14]. A detailed analysis showed that (14) agrees well with numerical calculations in almost the entire range of changes in the pumping rate from $r \ll r_{\text{th}}$ to $r \gg r_q$ (see section „Calculation results. . .“).

A similar result was obtained in [9]. However, the solution (14), as shown in [14], more accurately describes the behavior of a single-atom laser and can be used for a wider range of laser parameter values.

Some specifics of the coefficients in equation (3) (or (12)) should be noted:

(1) In case of a „good“ cavity regime $I_s \gg 1$, if conditions (9), (11) are met, the following approximated equalities are fulfilled:

$$I_0 \approx I_{+1} \approx I_{+2},$$

$$I_{-1} \approx I_s r/2\alpha, \quad I_{-2} \approx I_{\text{int}},$$

$$\frac{(I_{-1}-I_{-2})^2}{I_{-2}f_1} \approx \frac{\alpha(I_{-1}-I_{-2})}{I_{-2}} \approx Q_f. \quad (16)$$

Here, the expression for I_{-1} partially explains the limited scope of (14) — the impossibility of observing a field with an intensity greater than $I_s r/2$.

(2) In case of extremely strong atom-field coupling, i. e. at $c \to \infty$, for the roots of the polynomials, we have the following expressions:

$$I_0 = \frac{I_s(r+1)-1}{2},$$

$$I_{\pm1} = \frac{I_s(2r+1)-1 \pm |I_s-1|}{4},$$

$$I_{\pm2} = \frac{I_s r \pm \sqrt{(I_s-1)(I_s-3)}}{2}. \quad (17)$$

3.1.2. Approximated solution for Q-distribution

In the conditions in question (11) the roots of the polynomials and the coefficients in equation (13) are of the order of unity: $x_{00}, x_{ik} \sim 1$, $I_{sc}^{-3}b_{30}$, $I_{sc}^{-1}\tilde{b}_{31}$, $\tilde{b}_{32} \sim 1$.

The location of the large parameter λ in equation(13) allows to search for its approximate solution by considering the following second-order differential equation:

$$I_{sc}^{-1}\left(\tilde{b}_{32}x^2 + I_{sc}^{-1}\tilde{b}_{31}x\right)Q_0^{(2)}(x) + \beta(x-x_{41})(x-x_{42})Q_0^{(1)}(x) + I_{sc}(x-x_{51})(x-x_{52})Q_0(x) = 0. \quad (18)$$

This equation corresponds to the „unperturbed“ equation for the distribution P_0 (14). It is difficult to find a solution to equation (18) in the case of arbitrary laser parameters. In [23], the term with the second derivative was dropped in (18), which is partially justified because of the link between the characteristic scale and the large parameter $I_{sc} = \lambda/8$. Solving the remaining first-order equation gives the expected result:

$$Q_0(I) = N_0\,(I-I_{41})^{g_1}\,(I_{42}-I)^{g_2}\,e^{-I/\beta},$$

$$g_1 = -\frac{(I_{41}-I_{51})\,(I_{41}-I_{52})}{\beta\,(I_{41}-I_{42})},$$

$$g_2 = \frac{(I_{42}-I_{51})\,(I_{42}-I_{52})}{\beta\,(I_{41}-I_{42})}. \quad (19)$$

Here, the expression in the first parenthesis is always positive, since $I_{41} < 0$. In contrast to (14) the exponent decreases ($\beta > 0$). In the second parenthesis for the laser parameters under consideration we have $I_{42} \approx I_s r/2$, which is quite far from the area of significant change of the function Q.

The solution (19), in contrast to the solution (14), allowed us to describe the weak sub-Poissonian behavior of the single-atom laser ($Q_f \approx -0.05$, for $c > 200$, $r = c/5$) predicted by the linear theory (8) [12,14], and also reproduce the main results (see section „Calculation results. . .“) obtained earlier from (14).

As an observation, we also note the behavior of the polynomials' roots in the equation for Q-distribution. So, under the conditions described, the roots of the polynomials in (18) satisfy the following approximate equalities:

(1) In case of a „good“ cavity regime $I_s \gg 1$, if conditions (9), (11) are met, the following approximated equalities are fulfilled:

$$I_{31} \approx I'_{31} = -\frac{b_{31}}{b_{32}} \approx I_{42} \approx I_{52},$$

$$I_{41} \approx -I_s r/4, \quad I_{51} \approx I_{\text{int}},$$

$$\frac{(I_{41}-I_{51})^2}{I_{51}g_1} - 2 \approx \frac{\beta(I_{51}-I_{41})}{I_{51}} - 2 \approx Q_f. \quad (20)$$

(2) In case of extremely strong atom-field coupling ($c \to \infty$) it is interesting to compare the roots corresponding to the roots $I_{\pm2}$ in (17):

$$I_{51} = \frac{I_s r - \sqrt{(I_s+1)(I_s+3)}}{2},$$

$$I_{52} = \frac{I_s r + \sqrt{(I_s+1)(I_s+3)}}{2}. \quad (21)$$

3.2. „Linear“ characteristic scale

For the limiting case $c \to \infty$ it is needed to select another scale of the problem. It can be evaluated based on solutions (7), (8). Let's in (7), (8) $c \to \infty$, we get

$$I_{\text{int}}(r, I_s) = \frac{I_s(r-1)}{2}, \tag{22}$$

$$Q_f(r) = \frac{1}{(r-1)}. \tag{23}$$

From here we may select $I_{sc} = I_s r/2$ as a problem's characteristic scale.

3.2.1. „Unperturbed“ solution for P-distribution at $c \to \infty$

From the estimation of the characteristic scale of the problem, it is clear that the solution to equation (12) will be the function (14) found above, in which in all coefficients it is just needed to go to the limit $c \to \infty$. Using (17), we obtain

$$P_0(I) = \begin{cases} N_0\left(\frac{I_s(r+1)-1}{2} - I\right)\left(\frac{I_s r}{2} - I\right)^{\frac{I_s-3}{2}} e^I, & I \leqslant \frac{I_s r}{2}, \\ 0, & I > \frac{I_s r}{2}. \end{cases} \tag{24}$$

The solution (24) seemingly has a fairly simple structure, which, in particular, shows when the P-distribution can become negative. In fact, for $I_s < 1$ and $r > (1 - I_s)/I_s$, the first parenthesis in (24) changes its sign in the interval $(0, I_s r/2)$. Therefore, the sub-Poissonian statistics can be expected.

3.2.2. „Unperturbed“ solution for Q-distribution at $c \to \infty$

Let us now consider the equation (18). When $c \to \infty$ this equation, rewriting through the intensity variable, takes the form

$$(\tilde{b}_{31} I + I^2) Q_0^{(2)}(I) + (\tilde{b}_{40} + \tilde{b}_{41} I + 2I^2) Q_0^{(1)}(I) + (\tilde{b}_{50} + \tilde{b}_{51} I + I^2) Q_0(I) = 0, \tag{25}$$

$$\tilde{b}_{31} = -\frac{1}{2}\left(I_s(r+1) + 1\right),$$

$$\tilde{b}_{40} = -\frac{1}{4}(I_s + 3)\left(I_s(r+1) + 1\right),$$

$$\tilde{b}_{41} = -\frac{1}{2}\left(I_s(2r+1) + 1\right),$$

$$\tilde{b}_{50} = \frac{1}{4}\left(I_s^2(r^2-1) - 4I_s - 3\right), \quad \tilde{b}_{51} = -I_s r.$$

Solution of equation (25)(in contrast to (3)) can be searched in the standard way as a series $Q_0 = I^\alpha\left(c_0 + c_1 I + c_2 I^2 + \ldots\right)$ with corresponding defining equation for α [28,29]. Or use the integral relation between P- and Q-distributions [26,30]:

$$Q(I) = \int_0^\infty P(I') e^{-(I'+I)} I_0\left(2\sqrt{I'I}\right) dI', \tag{26}$$

where $I_n(x)$ — modified Bessel function of the first kind.

Without getting into specifics of simple calculations, let's write the solution:

$$Q_0(I) = N_0 I^{\frac{1-\nu}{2}}\left[\frac{(I_s r + 2\nu)}{\sqrt{2I_s rI}} I_\nu\left(\sqrt{2I_s rI}\right) + I_{\nu+1}\left(\sqrt{2I_s rI}\right)\right] e^{-I}, \tag{27}$$

where $\nu = (I_s + 1)/2$.

Note that when solving the second-order equation (25), two independent solutions are obtained. While physical solution (27) is obtained from a superposition of these solutions with the condition of boundedness at zero.

The solutions (24) and (27) were first obtained and investigated in [10] based on a system of equations for auxiliary probabilities. Note that these solutions do not take into account such a feature of a single-atom laser as the self-quenching effect, which is already evident from (22) and (23).

Thus, in this subsection it is shown that the case of the extremely strong atom-field coupling ($c \to \infty$) is included in the solution (14). And comparing equations (25) and (18) with each other explains why the solution of (19) cannot go into the solution of (27) at $c \to \infty$: removing the second derivative in (18) does not allow this. It is the first main result of this study.

For a more detailed analysis of solutions (24) and (27) see the original study. Here, for the sake of completeness, we will figure out three special cases. The first case is when $I_s \to 1$, also considered in [10], where the P-distribution behaves like a generalized function. The second case — $I_s \to 0$, whereas the product $I_s r$ remains constant. Third case — $I_s r \ll 1$.

3.2.3. Limit $I_s \to 1$

Let in expression (24) $I_s \to 1$. Seemingly, we get $P_0 = N_0 e^I$, but this is an erroneous result. Let's consider the solution (24), having rewritten it as below (only part for $I \leqslant I_s r/2$):

$$P_0(I) = N_0\left(\frac{I_s - 1}{2} + \frac{I_s r}{2} - I\right)\left(\frac{I_s r}{2} - I\right)^{\frac{I_s-3}{2}} e^I = N_0\left[\left(\frac{I_s r}{2} - I\right)^\varepsilon + \varepsilon\left(\frac{I_s r}{2} - I\right)^{\varepsilon-1}\right] e^I, \tag{28}$$

where $\varepsilon = (I_s - 1)/2$.

It can be seen from (28) that for $\varepsilon \to 0$, the second term in parentheses can be considered as a weak limit defining

Dirac δ-function. Thus,

$$P_0(I) = \begin{cases} \frac{1}{\pi(2e^{r/2}-1)}\left[1+\delta\left(\frac{r}{2}-I\right)\right]e^I, & I \leqslant \frac{r}{2}, \\ 0, & I > \frac{r}{2}. \end{cases} \quad (29)$$

where the normalization factor is explicitly written.

If we let in (27) I_s to unity and using the integral relation (26), it is easy to verify the correctness of the solution (29) with its limited domain of definition.

3.2.4. Limit $I_s \to 0$ at $I_s r = \text{const}$

Let's go to the limit $I_s \to 0$, in (24) and (27), while the product $I_s r$ will be fixed. Then

$$P_0(I) = N_0\left(\frac{I_s r - 1}{2} - I\right)\left(\frac{I_s r}{2} - I\right)^{-\frac{3}{2}} e^I, \quad (30)$$

$$Q_0(I) = N_0\left[\frac{I_s r}{\sqrt{2I_s rI}}\,\mathrm{sh}\left(\sqrt{2I_s rI}\right) + \mathrm{ch}\left(\sqrt{2I_s rI}\right)\right]e^{-I}. \quad (31)$$

These solutions for the case $I_s r = 1$ were analyzed by us earlier in [18,19].

3.2.5. Case $I_s r \ll 1$

Let's decompose the Bessel functions in solution (27) into a series with respect to a small parameter $I_s r$ and restrict ourselves to terms of the first order of smallness, then

$$Q_0(I) = \frac{1}{\pi(1 + I_s + 2I_s r)}\left[1 + I_s(r+1) + I_s rI\right]e^{-I}. \quad (32)$$

The remarkable feature of expression (32) is that it clearly reveals the Fermi statistics imposed by the atom on the cavity field. In fact, using (32) to calculate the average values of the operators $\hat{n}$ and $\hat{n}^2$, we obtain

$$\langle\hat{n}\rangle = \pi\int_0^\infty IQ_0(I)dI - 1 = \frac{I_s r}{1 + I_s + 2I_s r}, \quad (33)$$

$$\langle\hat{n}^2\rangle = \pi\int_0^\infty I^2 Q_0(I)dI - 3\langle\hat{n}\rangle - 2 = \frac{I_s r}{1 + I_s + 2I_s r}. \quad (34)$$

Thus,

$$\langle(\Delta\hat{n})^2\rangle = \langle\hat{n}^2\rangle - \langle\hat{n}\rangle^2 = \langle\hat{n}\rangle\left(1 - \langle\hat{n}\rangle\right). \quad (35)$$

The resulting dispersion of the number of photons corresponds to fluctuations in the number of particles for an ideal Fermi gas [31,32]. The single-atom laser is featuring such behavior because of both, the studied case of extremely strong coupling $c \to \infty$ and the condition of a small number of photons in the cavity $\langle\hat{n}\rangle \approx I_s r \ll 1$. The identification of Fermi features in the photon distribution is the second main result of this study.

3.3. Solutions for P- and Q-distributions at $r \ll r_{\text{th}}$, $r \gg r_q$

In case when the pumping parameter is much less than unity, which is equivalent to the inequality $r \ll r_{\text{th}}$, or much more than the cooperative parameter, which, in turn, is equivalent to $r \gg r_q$, the solution (14) is transformed to

$$P_0(I) = \frac{1}{\pi(a_{10}/a_{20})}\exp\left(-\frac{I}{(a_{10}/a_{20})}\right). \quad (36)$$

This result can be obtained directly from equation (3) by removing all terms in the polynomials containing I, I^2, I^3, i.e., assuming that the main changes in the P-distribution occur near $I \approx 0$.

The expression (36) describes the thermal distribution of photons in a mode with an average number of photons.

$$\langle\hat{n}\rangle = \frac{a_{10}}{a_{20}}. \quad (37)$$

For pumping parameter values below the threshold $r \ll r_{\text{th}}$, and provided that $c > 8$ and $I_s \gg 1$, solution (37) gives the result obtained earlier in [9]:

$$\langle\hat{n}\rangle \approx \frac{r}{1-r}. \quad (38)$$

Thus, this limiting case is also contained in solution (14).

For the values of the pumping parameter lying above the self-quenching point $r \gg r_q$ and under the same conditions $c > 8$ and $I_s \gg 1$, the solution (37) gives the following result [14]:

$$\langle\hat{n}\rangle \approx \frac{c}{r-c}. \quad (39)$$

The expressions for the average number of photons (38), (39), due to the fact that they correspond to the thermal distribution, represent an expression for the Mandel Q_f parameter in the corresponding regions. The latter has maxima (see „Calculation results. . .“), where solutions (38), (39) give a divergent result.

The corresponding Q-distribution for $r \ll r_{\text{th}}$ and $r \gg r_q$ we'll get from the equation (5), also neglecting all the terms with I, I^2, I^3 [23], then

$$b_{20}Q^{(3)}(I) + b_{30}Q^{(2)}(I) + b_{40}Q^{(1)}(I) + b_{50}Q(I) = 0. \quad (40)$$

Solving this equation we get

$$Q(I) = N_0\exp(aI), \quad (41)$$

where a is the real root of equation: $b_{20}x^3 + b_{30}x^2 + b_{40}x + b_{50} = 0$.

The average number of photons is given by the expression $\langle\hat{n}\rangle = -(a^{-1} + 1)$, which for the cases discussed above coincides with (38), (39).

At $r \to 0, \infty$ the root $a \approx -1$, i. e. in these limiting cases Q-function (similar as P-distribution (36)) describes the vacuum state of the mode — $Q(I) = e^{-I}/\pi$.

It is interesting to note that the solution (36) is a solution to the equation (3) for the case when $I_s \to \infty$ (the same

situation holds for Q-distribution). Let us $I_s \to \infty$ in relation to a_{10}/a_{20} in (36), we'll get the following value for the average number of photons:

$$\langle \hat{n} \rangle = \frac{r}{(1-r) + \frac{(r+1)^2}{c}}. \tag{42}$$

From (42) the mentioned above dependence of $\langle \hat{n} \rangle$ on r is clearly observed, in case when $r \ll r_{\text{th}} \approx 1$ or $r \gg r_q \approx c$. Note that (42) is valid not only in the conditions of the existence of a semiclassical solution $c > 8$, but also in the case when $c < 8$ for arbitrary values of r.

3.4. Solutions (14) and (19) related to the semiclassical intensity I_{int} and Mandel Q_f parameter

Solutions (14) and (19) describe the laser in a much wider range of problem parameter values than solutions (7), (8). They can be used for values of the pumping rate lying near the threshold, in the pre-threshold region, in the self-quenching region. These solutions describe more correctly the saturation yield and the transition to self-quenching.

It can be clearly shown that expressions for the semiclassical intensity (7) and the Mandel Q_f parameter (8) are included and derived from solutions (14) and (19) [14,23].

Let significant changes in P-distribution occur near the value of the variable intensity $I = I_{\text{int}}$. Then, providing for the approximate equalities (16), the pre-exponential factor in (14) is written approximately as

$$\left(1 - \frac{\triangle I}{\triangle I_{int}}\right)^{f_1} (I_{+1} - I)^{f_2} \approx \exp\left[f_1 \ln\left(1 - \frac{\triangle I}{\triangle I_{int}}\right)\right] \approx \exp\left[-\triangle I - \frac{1}{2}\frac{(\triangle I)^2}{I_{int} Q_f}\right], \tag{43}$$

where $\triangle I = I - I_{\text{int}}$, $\triangle I_{\text{int}} = I_{-1} - I_{\text{int}}$ and it was taken into account that $f_2 \approx 0$, $f_1 \approx \triangle I_{\text{int}} \approx I_{\text{int}} Q_f$. By substituting (43) in (14) we get

$$P_0(I) = N_0 \exp\left[-\frac{(I - I_{int})^2}{2D_p}\right], \tag{44}$$

where $D_p = I_{\text{int}} Q_f$ plays the role of dispersion of the Gaussian function about its mean value I_{int} and the restriction on P_0 in (14) can be removed.

Thus, the average number of photons and the photon-number dispersion are expressed in terms of semi-classical solutions as follows:

$$\langle \hat{n} \rangle = \pi \int_0^\infty I P_0(I)\, dI = I_{\text{int}}, \tag{45}$$

$$\langle (\Delta \hat{n})^2 \rangle = \langle \hat{n} \rangle + \pi \int_0^\infty (I - \langle \hat{n} \rangle)^2 P_0(I)\, dI = \langle \hat{n} \rangle + D_p = I_{\text{int}} [1 + Q_f]. \tag{46}$$

However, it should be noted that when $Q_f < 0$,,dispersion" becomes negative $D_p < 0$ and solution (44) with its unlimited domain of definition loses its meaning and cannot be used.

Similarly, we obtain the same Gaussian approximation for Q-distribution (19):

$$Q_0(I) = N_0 \exp\left[-\frac{(I - I_{\text{int}})^2}{2D_q}\right], \tag{47}$$

where $D_q = 1 + I_{\text{int}}(2 + Q_f)$ — the dispersion of the random variable I. We see that D_q is always positive. Then, for any possible Q_f , the expressions for averages are valid

$$\langle \hat{n} \rangle = \pi \int_0^\infty I Q_0(I)\, dI - 1 = I_{\text{int}}, \tag{48}$$

$$\langle (\Delta \hat{n})^2 \rangle = -(\langle \hat{n} \rangle + 1) + \pi \int_0^\infty (I - (\langle \hat{n} \rangle + 1))^2 Q_0(I)\, dI = -(\langle \hat{n} \rangle + 1) + D_q = I_{\text{int}} [1 + Q_f]. \tag{49}$$

Thus, the solution (47), in contrast to (44), can describe the sub-Poissonian statistics, which was well demonstrated in [23].

4. Comparison with a conventional laser

Let's add the inequality $I_s \gg 1$ to the previous limit transition $c \to \infty$. Then, the roots (17) will be simplified:

$$I_0 = I_{+1} = I_{+2} = \frac{I_s(r+1)}{2}, \quad I_{-1} = \frac{I_s r}{2}, \quad I_{-2} = \frac{I_s(r-1)+2}{2}, \tag{50}$$

and solution (14) takes the form

$$P_0(I) = \begin{cases} N_0 \left(\frac{I_s r}{2} - I\right)^{\frac{I_s}{2}-1} e^I, & I \leqslant \frac{I_s r}{2}, \\ 0, & I > \frac{I_s r}{2}. \end{cases} \tag{51}$$

The resulting expression (51) coincides with the solution for a conventional laser [26], P-distribution of which is also represented by a non-analytical function:

$$P_{cl}(I) = \begin{cases} N_0 \left(\frac{\mathcal{A}^2}{\mathcal{B}C} - I\right)^{\frac{\mathcal{A}}{\mathcal{B}}-1} e^I, & I \leqslant \frac{\mathcal{A}^2}{\mathcal{B}C}, \\ 0, & I > \frac{\mathcal{A}^2}{\mathcal{B}C}. \end{cases} \tag{52}$$

Here, $\mathcal{A}$ — linear amplification coefficient, $\mathcal{B}$ — self-saturation coefficient and C — resonator mode decay rate

(Appendix 2). And for a laser operating significantly above the threshold, (52) gives the following expressions for the intracavity intensity I_{cl} and Mandel Q_{cl} parameter:

$$I_{cl} = \frac{\mathcal{A}}{\mathcal{B}}\left(\frac{\mathcal{A}}{\mathcal{C}} - 1\right), \tag{53}$$

$$Q_{cl} = \frac{1}{\left(\frac{\mathcal{A}}{\mathcal{C}} - 1\right)}. \tag{54}$$

Note that in the limiting case considered here ($c \to \infty$), the expressions (53), (54) coincide with the corresponding expressions for a single-atom laser (22), (23).

The intracavity intensity (22) and the Mandel parameter (23) describe the behavior of a conventional laser [26,33] with a threshold dimensionless pumping value $r_{\text{th}} = 1$. The Mandel Q_f-parameter is always positive, i.e., the intracavity field is a super-Poissonian. At $r \gg 1$ $Q_f \approx 0$, i. e. the field statistics becomes a Poissonian.

The coincidence of P-distribution (51) with the corresponding distribution for a conventional laser (52) can be explained as follows. The limiting transition $c \to \infty$ may be interpreted as an increase in the number of atoms in the system [34–36]. The condition $I_s \gg 1$ ensures the accumulation of a large number of coherent photons in the mode that randomly leave this mode. Both of these factors erase the atom's individuality, which is already evident in the solutions (7), (8).

As mentioned in [26], the non-analytical behavior of $P_{cl}(I)$ (52) is explained by the presence of derivatives of all orders of $P_{cl}(I, \varphi, t)$ with respect to variables I and φ ($z = \sqrt{I}e^{i\varphi}$) in the appropriate non-stationary equation. It can be shown that in our case, the derivation of the equation (3) also faces the problem of derivatives of all orders. Therefore, it is possible that the limited domain of finding solution (24) can be understood in the same way as in the case of a conventional laser.

Thus, in this section, the relationship between a single-atom laser and a conventional laser with a macroscopic amount of emitters is found and explained. It is the third main result of this study.

5. Calculation results. Transition to the thresholdless regime

In Fig. 1 the results obtained with the help of solution (14) are presented. A characteristic square-law dependence of the average number of photons in the cavity mode on the pump parameter is visible. There are also two pronounced peaks for the Mandel Q_f parameter related to its behavior near the threshold pump rate and value of the pump rate corresponding to the self-quenching effect. For the pump rate values above r_{th} and below r_q, there is good agreement with the semiclassical solution (7) and solution (8).

The main dependences in Fig. 1 are related to the fact that higher value of coupling constant c entails both a natural rise of the photons number in the cavity mode and a shift of $r_{\max}$ and r_q. The latter is due to the fact that in order to destroy the stronger coupling „atom−field " and „capture" atom in the excited state, a stronger incoherent excitation of the atom shall be applied.

The same results can be obtained using an approximate solution for Q-distribution (19). However, for $r \ll r_{\text{th}}$ and $r \gg r_q$ solution (19) gives an erroneous result.

The Mandel Q_f parameter plotted using three solutions (14), (19), and (41), for the values of pump rate close to the classical threshold $r_{\text{th}} \approx 1$ is presented in Fig. 2, *a*. It can be seen that Q_f, plotted using (19), increases to unity at $r \to 0$ instead of tending to zero, describing the vacuum state. Such non-physical behavior is due to the fact that when (19) was obtained, the term containing the second derivative with respect to Q-distribution was neglected in the corresponding equation (18). It is the „loss of" of this term that distinguishes the solution (19) from the solution (14) providing correct result for P-distribution (see text after formula (18)). As can be seen from equation (40) for the function Q (its solution (41), as well as the solution (14), adequately delineates the approaching to the vacuum state of the mode), for small values of intensity variable, the term with the second derivative cannot be neglected ($b_{30} \sim I_s^2$). On the other hand, the found approximation (19) is able to describe the sub-Poissonian photon statistics Fig. 2, *b* predicted by the solution (8).

The behavior of the laser near the threshold is analyzed in Fig. 3. One can see that transition to a strong atom-field coupling leads to a decline in the threshold peak specific for the conventional laser. Fig. 3, *a*, *b* illustrates this transition in the case of a „good" cavity regime $I_s \gg 1$. It can be seen that the threshold doesn't disappear completely even in the limiting case of strong coupling $c \to \infty$ (Fig. 3, *c*).

The threshold peak starts to vanish completely after transition to the „bad " cavity regime $I_s \approx 1$. This behavior can be explained by revealing inequalities corresponding to the considered cases. Thus, for the strong coupling $c > I_s$ in conditions of a „good" cavity regime $I_s \gg 1$ the following inequalities are fulfilled $g > \gamma \gg \kappa$. Near the threshold $\Gamma \approx \gamma$ and the average number of photons in the mode is small $\langle \hat{n} \rangle \approx 1$. Then, on the photon lifetime $\tau_\kappa \sim \kappa^{-1}$, there will be many acts of both coherent atom-field interaction and spontaneous decay of the atom caused by the corresponding reservoir. By increasing the coupling $c \gg I_s$, the threshold peak will decrease, but due to the continued condition $I_s \gg 1$ will not disappear.

When transiting to the case of „bad" cavity regime $I_s \approx 1$ we have the following inequalities: $g \gg \gamma \approx \kappa$. In this case, the lifetime of the photon will practically coincide with the lifetime of the atom at both the upper and lower levels. This will ensure some order in the process of photon-atom interaction, which will lead to sub-Poissonian statistics, and consequently, to the disappearance of the threshold.

Thus, it is clear that the condition for the transition to a thresholdless regime of operation of a single-atom laser

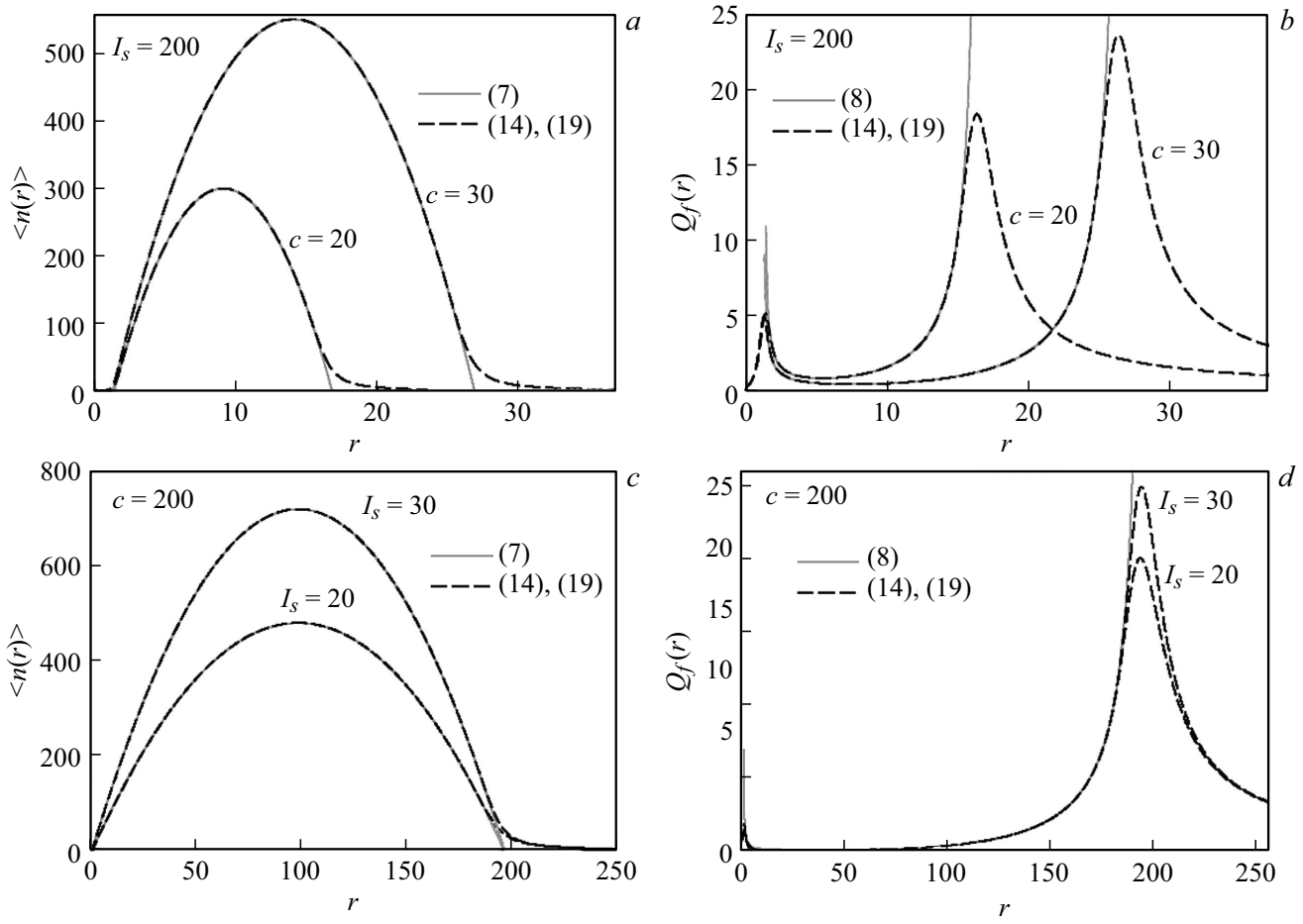

Figure 1. Average number of photons $\langle \hat{n} \rangle$ (a, c) and Mandel Q_f parameter (b, d) as a function of r. Dashed line — (14), (19). Grey solid line — (7), (8).

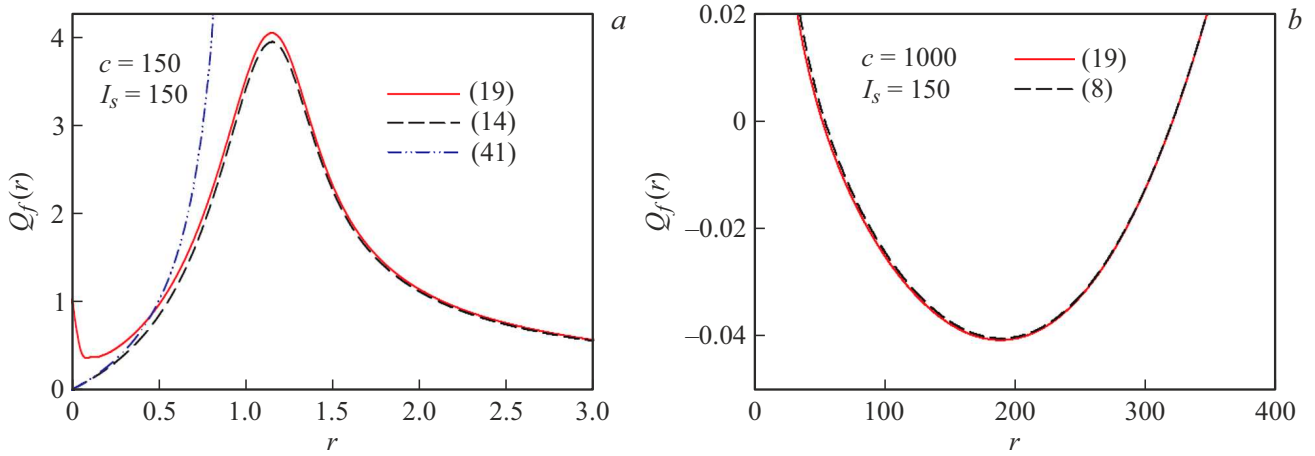

Figure 2. Mandel Q_f parameter as a function of r. (a) Comparison of calculations performed using solutions (14) — dashed line, (19) — solid line (41) — dotted line. (b) sub-Poissonian statistics, (19) — solid line, (8) — dashed line.

(generating under the conditions (11)) there cannot be only one inequality $c \gg I_s$ [12]. It shall be clarified by writing $c \gg I_s \approx 1$. It is the fourth main result of this study.

Figure 4 compares the behavior of a single-atom laser on two different characteristic scales of the problem — „square-law“ and „linear“. The plotted curves demonstrate a natural coincidence of the average number of photons for the pump

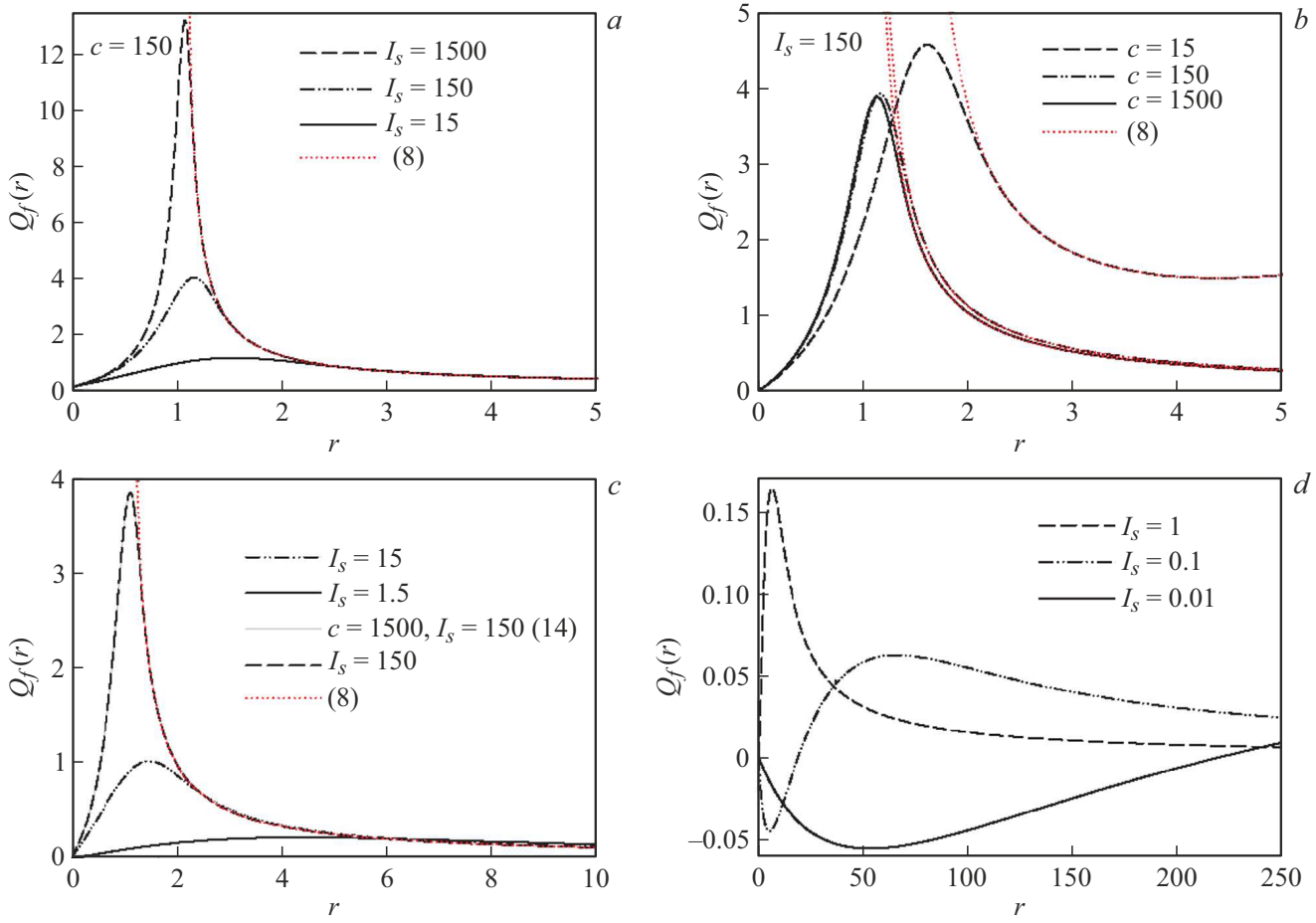

Figure 3. The behavior of a single-atom laser near a threshold. Mandel Q_f parameter as a function of r. Transition to the strong atom-field coupling $c > I_s$: (a) at fixed c; (b) at fixed I_s. (c,d) case of extremely strong atom-field coupling $c \to \infty$. Where there is no reference to the formula, the solution (14) is used for (a,b) and solution for (27) for (c,d).

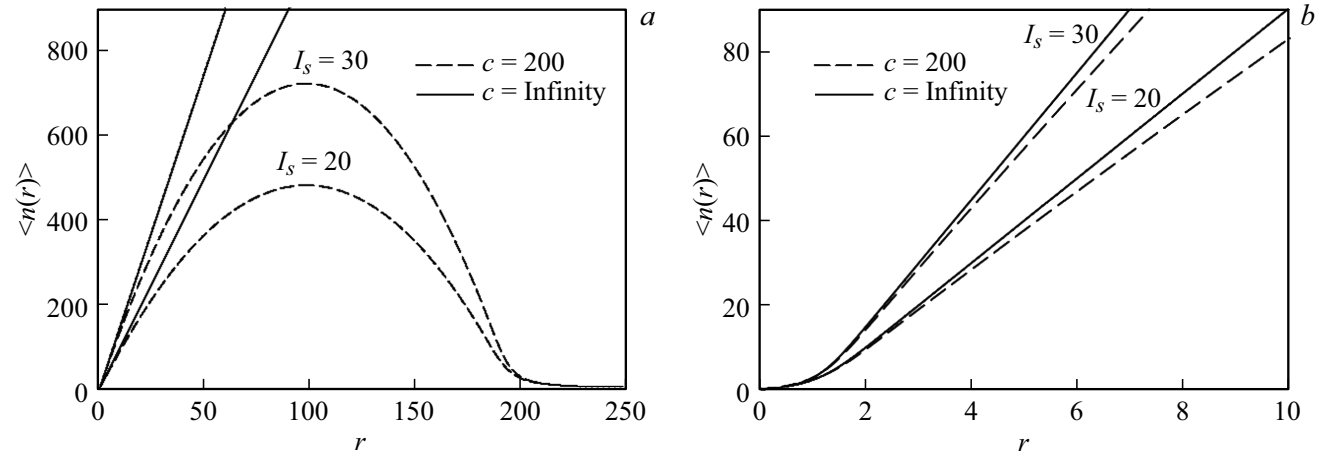

Figure 4. Average value of the photons number $\langle \hat{n} \rangle$ as a function r. Dashed line — (14), (19). Solid line — (24), (27).

values near the threshold and a significant discrepancy when reaching saturation.

At the end of this section we'd like to emphasize that for the considered single-atom laser model the minimum value of the Mandel parameter is $Q_f = -0.15$ [7,10,18]. Yet, for the conditions reviewed in this article (11), as seen from the obtained results (Fig. 2, b and Fig. 3, d), the minimal Mandel parameter is $Q_f \approx -0.05$.

6. Conclusion

The purpose of this work was to consider all known stationary solutions for a single-atom laser from a single position. Thus, it was shown that in the regime of existence of a semiclassical solution, a large parameter appears in the equations for phase-averaged P- and Q-distributions. The corresponding „unperturbed“ solutions of these equations contain all the known stationary solutions identified earlier.

In addition, several new results were obtained. The presence of fermionic features in the photon distribution for a single-atom laser operating in the regime of extremely strong coupling and a small number of photons in the cavity is clearly shown. The conditions are found when a single-atom laser begins to generate like a conventional laser, and the corresponding P-distribution coincide. The conditions for the transition to a thresholdless regime of operation of a single-atom laser in the regime of existence of a semiclassical solution have been clarified. For the same case, it was found that the minimum value of the Mandel parameter was $Q_f \approx -0.05$.

The approximate solutions described in the paper can be obtained only due to the large parameter in the equations: $cI_s \gg 1$. For the case $cI_s \approx 1$, when the Mandel parameter takes its lowest possible value for this model $Q_f \approx -0.15$, approximate solutions, as we know, have not yet been found.

In conclusion, we note that there's still high interest in the problem of a single-atom laser and related problems [37–45], where the effects associated with the interaction of a quantum field with single emitters are significant. And since the early 2000s, previously purely theoretical problems have become experimental, aimed at practical applications of [46–58], in particular, in problems related to quantum networks [59] and their safety [60].

Conflict of interest

There is no conflict of interest.

Appendix 1

Writing of polynomials (4) through coefficients a_{ik}:

$$p_0(I) = \left(a_{02}I^2 + a_{03}I^3\right),$$
$$p_1(I) = \left(a_{10} + a_{11}I + a_{12}I^2\right),$$
$$p_2(I) = \left(a_{20} + a_{21}I + a_{22}I^2\right). \quad \text{(A1)}$$

Coefficients a_{ik}:

$$a_{02} = \frac{1}{2}\left[1 - I_s\,(r+1)\right],\ a_{03} = 1;$$
$$a_{10} = \frac{cI_s^2 r}{4}\left[1 - I_s(r+1)\right],$$
$$a_{11} = \frac{1}{4}\left[9 - 2I_s(6(r+1)+c) + I_s^2(3(r+1)^2 + c(4r+2))\right],$$
$$a_{12} = \frac{1}{2}\left[7 - I_s(3(r+1)+2c)\right];$$
$$a_{20} = \frac{1}{4}\Bigg[6 - I_s(11(r+1)+3c) + 2I_s^2(3(r+1)^2+2c) + cI_s^3(r+1)\left[(r-1) - \frac{(r+1)^2}{c}\right]\Bigg],$$
$$a_{21} = \frac{1}{2}\left[3 - 4I_s(r+1) - I_s^2(2cr - (r+1)^2)\right],\ a_{22} = cI_s. \quad \text{(A2)}$$

Writing of polynomials (6) using coefficients b_{ik}:

$$q_0(I) = \left(b_{02}I^2 + b_{03}I^3\right),$$
$$q_1(I) = \left(b_{11}I + b_{12}I^2 + b_{13}I^3\right),$$
$$q_2(I) = \left(b_{20} + b_{21}I + b_{22}I^2 + b_{23}I^3\right),$$
$$q_3(I) = \left(b_{30} + b_{31}I + b_{32}I^2 + b_{33}I^3\right),$$
$$q_4(I) = \left(b_{40} + b_{41}I + b_{42}I^2\right),$$
$$q_5(I) = \left(b_{50} + b_{51}I + b_{52}I^2\right). \quad \text{(A3)}$$

Coefficients b_{ik}:

$$b_{02} = -\frac{1}{2}\left[1 + I_s(r+1)\right], \quad b_{03} = 1;$$
$$b_{11} = -3\left[1 + I_s(r+1)\right],\ b_{12} = \frac{1}{2}\left[7 - 3I_s(r+1)\right],\ b_{13} = 3;$$
$$b_{20} = -3\left[1 + I_s(r+1)\right],$$
$$b_{21} = \frac{1}{4}\left[-21 - 26I_s(r+1) + 3I_s^2(r+1)^2\right],$$
$$b_{22} = -3\left[-4 + I_s(r+1)\right], \quad b_{23} = 3;$$
$$b_{30} = \frac{1}{2}\left[-15 - 8I_s(r+1) + 3I_s^2(r+1)^2\right],$$
$$b_{31} = -\frac{1}{2}I_s\left[c(1 + I_s(r+1)) - (r+1)(-13 + 3I_s(r+1))\right],$$
$$b_{32} = \frac{1}{2}\left[23 + I_s(2c - 7(r+1))\right],\ b_{33} = 1; \quad \text{(A4)}$$

$$b_{40} = \frac{1}{4}\Big[-24 + I_s(r+1-3c) - I_s^3(r+1)(c+(r+1)^2) + I_s^2(8(r+1)^2 - c(3r+4))\Big],$$

$$b_{41} = \frac{1}{4}\Big[15 - 2I_s(c+10(r+1)) + I_s^2(5(r+1)^2 - 2c(2r+1))\Big],$$

$$b_{42} = \frac{1}{2}\left[7 + I_s(4c - 3(r+1))\right];$$

$$b_{50} = \frac{1}{4}\Big[-6 + I_s(5(r+1) - 3c) + I_s^3(r+1) \times (c(r-1) - (r+1)^2) + I_s^2(2(r+1)^2 - 4c)\Big],$$

$$b_{51} = \frac{1}{2}\left[3 - 4I_s(r+1) + I_s^2((r+1)^2 - 2cr)\right], \quad b_{52} = cI_s.$$

Appendix 2

P-distribution for a conventional laser P_{cl} satisfies with the following system of differential equations [26]:

$$\mathcal{A}\left(\frac{\partial}{\partial I} I - \frac{\partial}{\partial I} I \frac{\partial}{\partial I}\right) M(I) = \mathcal{C} \frac{\partial}{\partial I}\left(I P_{cl}(I)\right),$$

$$\left[1 - \frac{\mathcal{B}}{\mathcal{A}}\left(I\frac{\partial}{\partial I} - I\right)\right] M(I) = P_{cl}(I), \qquad \text{(A5)}$$

where $M(I)$ — additional probablity function. Laser parameters: $\mathcal{A}$ — linear amplification coefficient, $\mathcal{B}$ — self-saturation coefficient and $\mathcal{C}$ — cavity mode decay rate. $\mathcal{A}$ and $\mathcal{B}$ may be rewritten via the constant of atom-field coupling g, atomic relaxation constants $\gamma_\perp$, $\gamma_\parallel$ and effective pump rate r_a: $\mathcal{A} = 2g^2 r_a/(\gamma_\perp\gamma_\parallel)$, $\mathcal{B} = 4g^2\mathcal{A}/(\gamma_\perp\gamma_\parallel)$.

From the system of equations (A5) it is quite easy to get one equation for P_{cl}. Omitting elementary transformations, we obtain the following second-order differential equation:

$$\sum_{\nu=0}^{2} \tilde{p}_{2-\nu}(I) P_{cl}^{(\nu)}(I) = 0, \qquad \text{(A6)}$$

where the polynomial coefficients are expressed as

$$\tilde{p}_0(I) = \left(\tilde{a}_{01} I + \tilde{a}_{02} I^2 + \tilde{a}_{03} I^3\right),$$

$$\tilde{p}_1(I) = \left(\tilde{a}_{10} + \tilde{a}_{11} I + \tilde{a}_{12} I^2 + \tilde{a}_{13} I^3\right),$$

$$\tilde{p}_2(I) = \left(\tilde{a}_{20} + \tilde{a}_{21} I + \tilde{a}_{22} I^2\right). \qquad \text{(A7)}$$

Coefficients $\tilde{a}_{ik}$:

$$\tilde{a}_{01} = \mathcal{A}^3,$$

$$\tilde{a}_{02} = \mathcal{A}\mathcal{B}(\mathcal{A} - \mathcal{C}),$$

$$\tilde{a}_{03} = -\mathcal{B}^2\mathcal{C};$$

$$\tilde{a}_{10} = \mathcal{A}^3,$$

$$\tilde{a}_{11} = \mathcal{A}\left(\mathcal{A}\mathcal{C} - 3\mathcal{B}\mathcal{C} - \mathcal{A}^2\right),$$

$$\tilde{a}_{12} = \mathcal{B}\left(2\mathcal{A}\mathcal{C} - 2\mathcal{B}\mathcal{C} - \mathcal{A}^2\right),$$

$$\tilde{a}_{13} = \mathcal{B}^2\mathcal{C};$$

$$\tilde{a}_{20} = \mathcal{A}\left(\mathcal{A}\mathcal{C} - \mathcal{B}\mathcal{C} - \mathcal{A}^2\right),$$

$$\tilde{a}_{21} = 2\mathcal{A}\mathcal{B}\mathcal{C},$$

$$\tilde{a}_{22} = \mathcal{B}^2\mathcal{C}. \qquad \text{(A8)}$$

The equation (A6) is solved by using the non-analytical function (52) [26].

References

[1] Yi Mu, C.M. Savage. Phys. Rev. A, **46**, 5944 (1992). DOI: 10.1103/PhysRevA.46.5944

[2] G.S. Agarwal, S. Dutta Gupta. Phys. Rev. A, **42**, 1737 (1990). DOI: 10.1103/PhysRevA.42.1737

[3] S.Ya. Kilin, T.B. Karlovich. Opt. and spectr., **70**, 628 (1991). EDN: YTDGOT.

[4] C. Ginzel, H.J. Briegel, U. Martini, B.G. Englert, A. Schenzle. Phys. Rev. A, **48**, 732 (1993). DOI: 10.1103/PhysRevA.48.732

[5] T. Pellizzari, H. Ritsch. Phys. Rev. Lett., **72**, 3973 (1994). DOI: 10.1103/PhysRevLett.72.3973

[6] M. Loffler, G.M. Meyer, H. Walther. Phys. Rev. A, **55**, 3923 (1997). DOI: 10.1103/PhysRevA.55.3923

[7] A.V. Kozlovsky, A.N. Oraevsky. ZhETF, (in Russian). **115**, 1210 (1999). DOI: 10.1134/1.558842

[8] B. Jones, S. Ghose, J.P. Clemens, P.R. Rice, L.M. Pedrotti. Phys. Rev. A, **60**, 3267 (1999). DOI: 10.1103/PhysRevA.60.3267

[9] T.B. Karlovich, S.Ya. Kilin. Opt. and spectr., **91**, 374 (2001). EDN: YSPNZR, DOI: 10.1134/1.1405210

[10] S.Ya. Kilin, T.B. Karlovich. ZhETF, **122** (in Russian). 933 (2002). EDN: YSSXIL. DOI: 10.1134/1.1528672

[11] T.B. Karlovich. Opt. i spektr., **111**, 758 (in Russian). (2011). EDN: OJGTRT. DOI: 10.1134/S0030400X11120113

[12] N.V. Larionov, M.I. Kolobov. Phys. Rev. A, **84**, 055801 (2011). DOI: 10.1103/PhysRevA.84.055801

[13] S.Ya. Kilin, A.B. Mikhalychev. Phys. Rev. A, **85**, 063817 (2012). DOI: 10.1103/PhysRevA.85.063817

[14] N.V. Larionov, M.I. Kolobov. Phys. Rev. A, **88**, 013843 (2013). DOI: 10.1103/PhysRevA.88.013843

[15] E.N. Popov, N.V. Larionov. Proc. SPIE, **9917**, 99172X (2016). DOI: 10.1117/12.2229228

[16] V. Stefanov, S.Y. Kilin. Nonlinear Phenomena in Complex Systems, **22**, 64 (2019). EDN: ZIJQTJ.

[17] V.A. Bobrikova, R.A. Khachatryan, K.A. Barantsev, E.N. Popov. Opt. i spektr., **127**, 976 (in Russian). DOI: 10.21883/OS.2019.12.48695.39-19
[18] N.V. Larionov. Proc. IEEE Int. Conf. on Electrical Engineering and Photonics (EExPolytech), 265 (2020). DOI: 10.1109/EExPolytech50912.2020.9243955
[19] N.V. Larionov. J. Phys.: Conf. Ser., **2103**, 012158 (2021). DOI: 10.1088/1742-6596/2103/1/012158
[20] B. Parvin. Eur. Phys. J. Plus, **136**, 728 (2021). DOI: 10.1140/epjp/s13360-021-01720-5
[21] D.B. Horoshko, Chang-Shui Yu, S.Ya. Kilin. J. Opt. Soc. Amer. B, **38**, 3088 (2021). DOI: 10.1364/JOSAB.436004
[22] A.B. Mikhalychev, S.V. Vlasenko, S.Ya. Kilin. Phys. Rev. A, **105**, 063723 (2022). DOI: 10.1103/physreva.105.063723
[23] N.V. Larionov ZhETF, **161** (166), 2022 (in Russian). DOI: 10.31857/S004445102202002X
[24] B. Parvin. Annals of Physics, **471**, 169832 (2024). DOI: 10.1016/j.aop.2024.169832
[25] A.H. Nayfeh. *Perturbation Methods* (N.Y., Wiley. Interscience, 2000).
[26] M.O. Skalli, M.S. Zubairi. *Kvantovaya optika* edited by V.V. Samarceva (Fizmatlit, M., 2003) (in Russian).
[27] H.J. Carmichael. *Statistical methods in quantum optics 1: master equations and Fokker-Planck equations* (Springer Science and Business Media, 2013).
[28] E. Madelung. *Matematicheskiy apparat physiki.* , edited by V.I. Levin, 2-d ed., ster. (M., Nauka, 1968) (in Russian).
[29] A.D. Polyanin, V.F. Zaitsev. *Handbook of Exact Solutions for Ordinary Differential Equations*, 2nd ed. (Boca Raton.London: Chapman and Hall/CRC Press, 2003).
[30] B. Daeubler, H. Risken, L. Schoendoff. Phys. Rev. A, **48**, 3955 (1993). DOI: 10.1103/PhysRevA.48.3955
[31] A.I. Anselm. *Osnovy statisticheskoy fiziki i termodinamiki* (Lan', SPb, 2022).
[32] D.F. Smirnov, A.S. Troshin. UFN, **153**, 233 (1987). DOI: 10.3367/UFNr.0153.198710b.0233
[33] L. Mandel, E. Volf. *Opticheskaya kogerentnost i kvantovaya optika* (Fizmatlit, M., 2000) (in Russian).
[34] M.O. Scully, W.E. Lamb. Physical Review, **159**(2), 208 (1967). DOI: 10.1103/physrev.159.208
[35] M.G. Raizen, R.J. Thompson, R.J. Brecha, H.J. Kimble, H.J. Carmichael. Phys. Rev. Lett., **63**, 240 (1989). DOI: 10.1103/PhysRevLett.63.240
[36] R.B. Levien, M.J. Collett, D.F. Walls. Phys. Rev. A, **47**, 5030 (1993). DOI: 10.1103/physreva.47.5030
[37] S. Ashhab, J.R. Johansson, A.M. Zagoskin, F. Nori. New J. Physics, **11**, 023030 (2008). DOI: 10.1088/1367-2630/11/2/023030
[38] S.O. Tarasov, S.N. Andrianov, N.M. Arslanov, S.A. Moiseev. Bulletin of the Russian Academy of Sciences: Seriya fizicheskaya, **82**(8), 1148 (2018) (in Russian). DOI: 10.3103/S1062873818080415
[39] E.N. Popov, V.A. Reshetov. Pisma v ZhETF, **111**, 846 (2020). DOI: 10.31857/S1234567820120113
[40] A.A. Sokolova, G.P. Fedorov, E.V. Il'ichev, O.V. Astafiev. Phys. Rev. A, **103**, 013718 (2021). DOI: 10.1103/PhysRevA.103.013718
[41] Y.-W. Lu, W. Li, R. Liu, Y. Wu, H. Tan, Y. Li, J.-F. Liu. Phys. Rev. B, **106**, 115434 (2022). DOI: 10.1103/PhysRevB.106.115434
[42] S. Vlasenko, A. Mikhalychev, S. Pakniyat, G. Hanson, A. Boag, G. Slepyan, D. Mogilevtsev. Advanced Quantum Technologies, **6**, (2023). DOI: 10.1002/qute.202300060
[43] A. Dey, A. Pal, S.D. Gupta, B. Deb. Phys. Scr., **98**, 065527 (2023). DOI: 10.1088/1402-4896/acd4f5
[44] A.S. Kuraptsev, I.M. Sokolov. Phys. Rev. A, **112**, 013702 (2025). DOI: 10.1103/s85r-vx8t
[45] E.N. Popov, A.I. Trifanov, M.A. Moskalenko, V.A. Reshetov. Nanosystems: Physics, Chemistry, Mathematics, **16**, 176 (2025). DOI: 10.17586/2220-8054-2025-65-2-176-182
[46] J. McKeever, A. Boca, A.D. Boozer, J.R. Buck, H.J. Kimble. Nature, **425**, 268 (2003). DOI: 10.1038/nature01974
[47] K.M. Birnbaum, A. Boca, R. Miller, A.D. Boozer, T.E. Northup, H.J. Kimble. Nature, **436**, 87 (2005). DOI: 10.1038/nature03804
[48] D. Englund, A. Faraon, I. Fushman, N. Stoltz, P. Petroff, J. Vuckovic. Nature, **450**, 857 (2007). DOI: 10.1038/nature06234
[49] M. Nomura, N. Kumagai, S. Iwamoto, Y. Ota, Y. Arakawa. Opt. Express, **17**, 15975 (2009). DOI: 10.1364/OE.17.015975
[50] M. Nomura, N. Kumagai, S. Iwamoto, Y. Ota, Y. Arakawa. Nature Physics, **6**, 279 (2010). DOI: 10.1038/nphys1518
[51] F. Dubin, C. Russo, H. Barros, A. Stute, C. Becher, P. Schmidt, R. Blatt. Nat. Phys., **6**, 350 (2010). DOI: 10.1038/nphys1627
[52] A. Reiserer, G. Rempe. Rev. Mod. Phys., **87**, 1379 (2015). DOI: 10.1103/RevModPhys.87.1379
[53] C. Gies, F. Gericke, P. Gartner, S. Holzinger, C. Hopfmann, T. Heindel, J. Wolters, C. Schneider, M. Florian et al. Phys. Rev. A, **96**, 023806 (2017). DOI: 10.1103/PhysRevA.96.023806
[54] M. Mantovani, A.D. Armour, W. Belzig, G. Rastelli. Phys. Rev. B, **99**, 045442 (2019). DOI: 10.1103/PhysRevB.99.045442
[55] N. Tomm, S. Mahmoodian, N.O. Antoniadis, et al. Nat. Phys., **19**, 857 (2023). DOI: 10.1038/s41567-023-01997-6
[56] A.A. Sokolova, D.A. Kalacheva, G.P. Fedorov, O.V. Astafiev. Phys. Rev. A, **107**, L031701 (2023). DOI: 10.1103/PhysRevA.107.L031701.
[57] R. Sett, F. Hassani, D. Phan, S. Barzanjeh, A. Vukics, J.M. Fink. PRX Quantum, **5**, 010327 (2024). DOI: 10.1103/PRXQuantum.5.010327
[58] Z. Wang, S. Guan, G. Teng, et al. Quantum Front, **4**, 10 (2025). DOI: 10.1007/s44214-025-00083-7
[59] S. Ritter, C. Nolleke, C. Hahn et al. Nature, **484**, 195 (2012). DOI: 10.1038/nature11023
[60] I.N. Kartsan, V.S. Averyanov. Zaschita informatsii. Inside, **3** (111), 50 (2023). EDN: EQZKRC

Translated by T.Zorina